CrossMark

ORIGINAL ARTICLE

Variants and pitfalls on radioiodine scans in pediatric patients with differentiated thyroid carcinoma

Mohamed Mostafa[1] · Reza Vali[1] · Jeffrey Chan[1] · Yusuaf Omarkhail[1] · Amer Shammas[1]

Abstract

Background Potentially false-positive findings on radioiodine scans in children with differentiated thyroid carcinoma can mimic functioning thyroid tissue and functioning thyroid carcinomatous tissue. Such false-positive findings comprise variants and pitfalls that can vary slightly in children as compared with adults.

Objective To determine the patterns and frequency of these potential false-positive findings on radioiodine scans in children with differentiated thyroid carcinoma.

Materials and methods We reviewed a total of 223 radioiodine scans from 53 pediatric patients (mean age 13.3 years, 37 girls) with differentiated thyroid carcinoma. Focal or regional activity that likely did not represent functioning thyroid tissue or functioning thyroid carcinomatous tissue were categorized as variants or pitfalls. The final diagnosis was confirmed by reviewing the concurrent and follow-up clinical data, correlative ultrasonography, CT scanning, serum thyroglobulin and antithyroglobulin antibody levels. We calculated the frequency of these variants and pitfalls from diagnostic and post-therapy radioiodine scans.

Results The most common variant on the radioiodine scans was the thymic activity (24/223, 10.8%) followed by the cardiac activity (8/223, 3.6%). Salivary contamination and star artifact, caused by prominent thyroid remnant, were the most important observed pitfalls.

Conclusion Variants and pitfalls that mimic functioning thyroid tissue or functioning thyroid carcinomatous tissue on radioiodine scan in children with differentiated thyroid carcinoma are not infrequent, but they decrease in frequency on successive radioiodine scans. Potential false-positive findings can be minimized with proper knowledge of the common variants and pitfalls in children and correlation with clinical, laboratory and imaging data.

Introduction

Radioiodine scanning has an important role in the management of differentiated thyroid cancer [1–5]. Radioiodine scans can detect residual functioning thyroid tissue and functioning thyroid carcinomatous tissue with high specificity and accuracy. However, radioiodine scans sometimes express patterns representing variants or pitfalls. These variants and pitfalls can be sources of false-positive findings for functioning thyroid tissue or functioning thyroid carcinomatous tissue. Review of the literature shows many retrospective studies, case reports and reviews describing these variants and pitfalls [1, 4, 6–9]. Consequently these potential false-positive findings can influence treatment decisions including dose adjustment of radioiodine therapy, and surveillance and prognosis of the differentiated thyroid carcinoma. Few studies on this topic have focused on children. In children, particularly adolescents, differentiated thyroid carcinoma has relatively better prognosis and lesser incidence of mortality than in adults [10]. Further, the unique prevalence of certain pathological conditions and artifacts like thymic activity and radioiodine contamination in children increases the significance of this

✉ Mohamed Mostafa
Mrazek12003@yahoo.com

1 Nuclear Medicine Division, Department of Medical Imaging, The Hospital for Sick Children, University of Toronto, 555 University Avenue, Toronto, Ontario M5G 1X8, Canada

study. It is essential to minimize misinterpretation of findings on radioiodine scans to avoid unnecessary radioiodine therapy. Proper and accurate interpretation of radioiodine scans is important to avoid further radiation exposure in children from unnecessary radioiodine therapy or the addition of ionizing radiation-based imaging procedures, particularly CT, or further investigation with MRI. The pediatric population is more vulnerable to radiation-induced cancers because of the greater cell division in developing tissues and longer expected lifetime of children (which increases the probability for more accumulated damage) [11, 12].

The purpose of this study was to review radioiodine scans in children and young adults, younger than 18 years, in order to determine the frequency of variants and pitfalls in this specific age group to help avoid misinterpretation and minimize unnecessary treatment and radiation exposure.

Materials and methods

Study population

This retrospective study was approved by our institutional research and ethics board. We reviewed a total of 223 radioiodine scans in 53 children with differentiated thyroid carcinoma after searching the database at the Hospital for Sick Children from Jan. 1, 2000, through Nov. 20, 2014. The children included 37 girls and 16 boys, with a mean age ± standard deviation (SD) of 13.3 ± 2.3 years (range, 9–17 years at initial scanning). All children, included in the study, had near-total thyroidectomy before scanning. The histopathological diagnosis in 50 children was papillary thyroid carcinoma, including the follicular variant of papillary carcinoma; the remaining 3 children were diagnosed as follicular carcinoma.

Radioiodine scans

All children followed iodine restriction in their diet for at least 7 days and stopped thyroid hormone replacement therapy for 2–4 weeks and avoided any iodine-containing medications and contrast material for at least 4–6 weeks prior to scanning. All children had serum thyroid stimulating hormone (TSH) levels ≥40 mIU/L (normal range: 0.73 to 4.09 mIU/L) prior to radioiodine administration.

Iodine-123 sodium iodide (NaI) scans were acquired 24 h after administration of 3–11 MBq (0.08–0.3 mCi). For I-131 scans, the diagnostic whole-body scans commenced 48 h after the administration of 148 MBq (4 mCi) of I-131 NaI, while the post-therapy whole-body scans were performed within 7–10 days after therapeutic radioiodine administration. The therapeutic radioiodine doses ranged from 1,091.5 to 7,400 MBq (29.5–200 mCi). Images were acquired using a dual-head gamma camera equipped with a low-energy high-resolution or pinhole collimators for I-123 NaI scans or high-energy collimators for I-131 NaI whole-body radioiodine scans.

For I-123 scans, 1- to 2-min anterior planar and 2- to 5-min pinhole-collimated images for the neck and upper chest were acquired. Right and left anterior oblique neck and anterior chest views were acquired in nine children. As per protocol of the Hospital for Sick Children, 10-min images were acquired in cases of low count rate.

The standard views for procedures utilizing I-131 included anterior and posterior whole-body images, with a 256 × 1,024 matrix size and a zoom of 1.0 at a speed of 15 min/meter, in addition to spot right and left lateral views of the head. Spot views of any compartment of the torso or extremities were acquired for some children for further verification or after thorough cleansing of the skin when contamination was suspected. Spot views of the neck, chest and upper abdomen were sometimes needed after the child drank water to wash upper gastrointestinal activity. For all spot views, a 256 × 256 matrix size, zoom of 1.0 and acquisition time of 10 min were applied.

Data analysis

Radioiodine scans were independently reviewed by two nuclear medicine physicians (M.M. and R.V., each with more than 10 years of experience in nuclear medicine) for findings including functioning thyroid tissue or functioning thyroid carcinomatous tissue, physiological radiopharmaceutical distribution, and abnormal activity patterns. In the case of discrepancy, a third nuclear medicine physician (A.S.) with 10 years of post-fellowship experience was called upon to review and reach consensus. Any focal activity other than the normal bio-distribution of iodine was recorded. The findings were then categorized into functioning thyroid tissue or functioning thyroid carcinomatous tissue, variants and pitfalls. Categorization was made in correlation with the clinical data, corresponding anatomical imaging (US or CT scan), the correlative serum levels of thyroglobulin and anti-thyroglobulin antibodies, as well as follow-up whole-body radioiodine scans. Variants were considered when the depicted focal or regional radioactivity pattern was expressed as physiological or pathological radioiodine accumulation that did not contribute to functioning thyroid tissue or functioning thyroid carcinomatous tissue uptake (e.g., thymic activity or retained activity caused by salivary gland obstruction). The well-known patterns of physiologically distributed radioiodine (e.g., in the urinary bladder, liver uptake after radioiodine therapy scan) were not considered variants. We defined the pitfall as the in vitro technical artifact on radioiodine scan that could be misinterpreted as functioning thyroid tissue or functioning thyroid carcinomatous tissue (e.g., radioiodine contamination or star artifact).

Results

We reviewed a total of 223 radioiodine scans from 53 children (average 4 scans per child, range 1–7). The scan set contained 45 I-123 scans (all done after thyroidectomy and before radioiodine therapy as the initial scans), 111 I-131 diagnostic whole-body scans (for follow-up or surveillance) and 67 I-131 post-therapy whole-body scans (7–10 days after therapeutic radioiodine dose) (Fig. 1). We identified 92 potential false-positive findings, including 63 variants and 29 pitfalls (Table 1; Figs. 1, 2, and 3). Thymic activity was the most frequently identified variant among all radioiodine scans (24/223) and represented 13.5% (24/178) of the whole-body radioiodine scans (Fig. 4). Among cases of thymic activity, 25.3% (17/67) findings of thymic uptake were revealed on post-therapy whole-body scans and 6.3% (7/111) were shown on diagnostic whole-body scans. Interestingly, the thymic activity faded over time in two children, as seen on follow-up whole-body radioiodine scans (Fig. 2). At least in some cases, this is probably a result of different doses of radioiodine administered in diagnostic iodine scans versus post-therapy iodine scans. Cardiac silhouette (8/223) was the second most frequent variant on whole-body radioiodine scans (Fig. 3). Specifically, slight cardiomegaly was found in two diagnostic whole-body scans of one child. Pulmonary activity (basal or diffuse) - in the absence of anatomical or biochemical evidence of pulmonary metastases - was the third most common variant. Single-photon emission computed tomography (SPECT)/CT was useful to differentiate pulmonary activity and true pulmonary metastases (Fig. 5). Among the pulmonary activity variants, three chest CT scans showed bronchiectatic changes. In all those cases, no evidence of thyroid carcinomatous metastases was revealed upon review of the subsequent follow-up whole-body radioiodine scans, nor was such evidence found in the corresponding thyroglobulin profile in three other children. The remaining variants are detailed in Table 1.

Pitfalls including salivary, sweat and urine contamination (23/223) and star artifact (6/223; Fig. 6) were also considered to be significant sources of potential false-positive findings in children with differentiated thyroid carcinoma. Contamination was demonstrated by changing or disappearing activity after changing the gown or cleansing. Salivary contamination was noted on the fingers or the gown covering the upper trunk, particularly the shoulders. Sweat contamination was noted in the axillary regions, while urinary contamination activity was typically demonstrated in the lower trunk and lower extremities. Almost all the pitfalls (28 among 29) were observed on whole-body radioiodine scans, and the remaining one, which was salivary contamination, was noted on one I-123 radioiodine scan. The remaining 3 cases of salivary contamination were noted on the second (n=2) and the third (n=1) whole-body radioiodine scans.

On reviewing trends in the frequency of potential false-positive findings on whole-body radioiodine scans (n=178), the highest frequency was observed with the first whole-body radioiodine scan, and this decreased on successive follow-up whole-body radioiodine scans (Fig. 7).

Discussion

Accurate interpretation of radioiodine scans can result in avoidance of unnecessary radioiodine therapy. Because of the complex systemic distribution of iodine within the body, it is not uncommon to see artifacts on radioiodine scans, and

Fig. 1 Flow chart shows potential false-positive findings for functioning thyroid tissue or functioning thyroid carcinomatous tissue on 223 radioiodine scans of 53 children with differentiated thyroid cancer
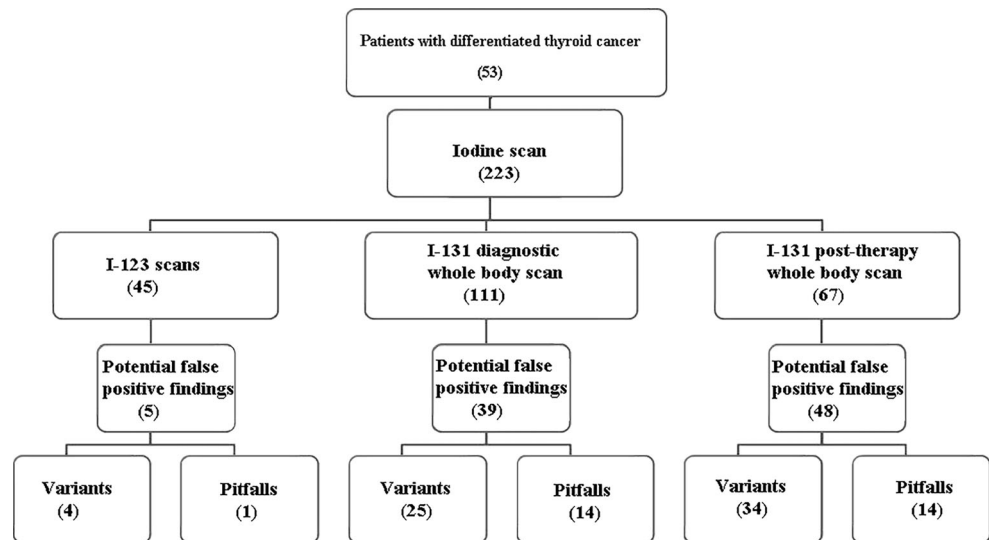
Table 1 Potential false-positive findings depicted on radioiodine scans of children with differentiated thyroid cancer

	I-123 scans n=45		I-131 dWBSs n=111		I-131 Rx WBSs n=67		Total RISs n=223		Verification of potential false-positive findings
	No	(%)	No	(%)	No	(%)	No	(%)	
Paranasal sinuses	1	(2.2)	1	(0.9)	1	(1)	3	(1)	Maxillary sinuses activity on two subsequent I-123 and post-therapy scans of one child with radiologic picture of bilateral maxillary sinusitis (opacities). Bilateral symmetrical activity, likely in ethmoidal sinuses, appeared on follow-up dWBS of one child whose serum Tg level was <2 ng/ml. Such activity disappeared on subsequent dWBS without interval radioiodine therapy.
Asymmetrical hot nose	2	(4.4)	1	(0.9)	2	(3)	5	(2.2)	Nose piercing in 2 girls.
Prominent salivary gland	0	(0)	3	(2.7)	2	(3)	5	(2.2)	Concurrent ultrasonography revealed stone in two children with sequential RxWBSs and dWBSs, and was suggestive of asymmetrical parotid sialadenitis in a third child; follow-up serum Tg level was <1.5 ng/ml in all of these cases.
Esophageal activity (saliva, acid or esophagitis)	1	(2.2)	1	(0.9)	0	(0)	2	(0.8)	In one child, the focal activity appeared on initial I-123 WBS and follow-up dWBS but was not present on RxWBS. The activity was demonstrated in the posterior mediastinum (in continuation with gastric activity), in a child with T1a-PTC. The activity demonstrated little change with water drinking. No enlarged mediastinal or cervical lymph nodes were seen on CT. The serum Tg level done simultaneously with the dWBS was <1.5 ng/ml.
Thymic activity	0	(0)	7	(6.3)	17	(25.3)	24	(10.8)	Two thymic activity patterns were elicited on initial WBSs of two children; two on two dWBSs of one child and three on three dWBSs of one child (became fainter on subsequent scans); three on subsequent RxWBSs of one child. The thymus was identified as "standard inverted Y shape, or V shape" on WBRIS and corresponding chest CT, which did not show enlarged mediastinal LNs within 6-week interval from four WBRISs (Fig. 2).
Cardiac activity	0	(0)	2	(1.8)	6	(9)	8	(3.6)	The cardiac silhouette (Fig. 3) was identified in consensus and in correlation with the concurrent CT.
Pulmonary activity	0	(0)	2	(1.8)	3	(4.5)	5	(2.2)	Pulmonary activity appeared on initial dWBSs (2 scans of two children); follow-up dWBS showed diffuse pulmonary activity, which was not apparent on RxWBS. The corresponding serum Tg level was <3 ng/ml. For RxWBSs, three scans of two children showed bilateral lung uptake not shown on dWBS prior to therapy. For all procedures, the concurrent chest CT did not show evidence of pulmonary metastases, with congruent bronchiectatic changes on three scans.
Extravesical urinary activity	0	(0)	2	(1.8)	2	(3)	4	(1.8)	Variable along the course of the urinary tract, two located in the renal pelvis. Correlative imaging modalities (abdominal US or CT) did not show corresponding abnormalities.
Arthropathies	0	(0)	2	(1.8)	0	(0)	2	(0.8)	One child with PTC had concurrent ipsilateral pain in the TMJ on mastication; the focus was on dWBS done 6 months after radioiodine ablation (was not apparent on the prior post-ablative RxWBS). Another child experienced mild right wrist pain, showed abnormal regional activity only at the right wrist on dWBS. All children had stimulated Tg level <1.5 ng/ml.
Stress fracture	0	(0)	3	(2.7)	0	(0)	3	(1)	Of two children with PTC, one presented with pain in the right distal 4th finger. The second (a hockey player) showed focal activity in the right distal thigh on two dWBS within 6-month interval. The two children had unremarkable radiography and stress fracture was suggested. Serum Tg level declined with time without intervening radioiodine therapy.
Knee osteochondritis	0	(0)	1	(0.9)	1	(1)	2	(0.8)	Focal unilateral anterior knee activity was seen on two successive scans within 6 months of a soccer player with PTC with normal bony architecture on plain radiograph. Such focal activity was the only abnormal activity on dWBS and disappeared on follow-up. Patellar tenderness was elicited.
Total variants	4	(8.8)	25	(22.5)	34	(50.7)	63	(28.3)	

CT computed tomography, *DTC* differentiated thyroid carcinoma, *I-131 dWBS* diagnostic I-131 whole-body scans, *I-131 RxWBS* post-therapeutic I-131 whole-body scan, *LN* lymph node, *PTC* papillary thyroid carcinoma, *RIS* radioiodine scan, *Tg* thyroglobulin, *TMJ* temporomandibular joint, *US* ultrasonography, *WBRIS* whole-body radioiodine scan, *T1a* tumor < 1 cm and limited to the thyroid
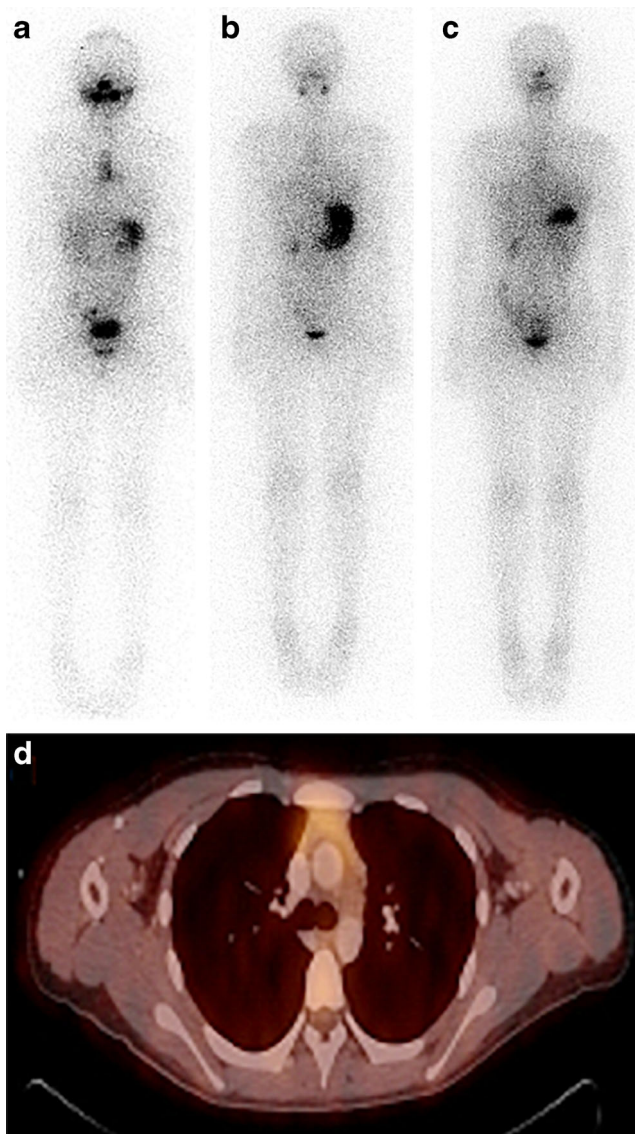
Fig. 2 Thymic activity on post-therapy whole-body scan (**a**) in a 13-year-old girl with papillary thyroid carcinoma. **b, c** The thymic activity fades on subsequent diagnostic whole-body scan done 6 months (**b**) and 18 months (**c**) later. The stimulated serum thyroglobulin (Tg) levels were 1.5 ng/ml and 0.9 ng/ml, corresponding to the latter two diagnostic whole-body scans. **d** The thymus is demonstrated on a corresponding axial chest positron emission tomography (PET)/CT scan 6 weeks prior to radioiodine therapy

Fig. 3 Cardiac activity. Two post-therapy whole-body radioiodine scans with 1-year interval in a 13-year-old girl with papillary thyroid carcinoma, metastatic to the cervical and superior mediastinal lymph nodes, show cardiac blood pool activity. The cardiac blood pool activity is more prominent on the initial (**a**) than on the subsequent (**b** and **c**) post-therapy scans. Bulky functioning thyroid carcinomatous tissue is noted on the initial post-therapy whole-body scan

these artifacts can be challenging for physicians on reviewing the scans [9]. These challenges increase with radioiodine scans in children because the addition of CT scanning would increase the radiation exposure and potential interference of contrast material with radioiodine uptake by functioning thyroid tissue or functioning thyroid carcinomatous tissue.

Overall, 92 potential false-positive findings were found in 223 radioiodine scans (41.3%) of 53 children with differentiated thyroid carcinoma. Considering this high prevalence of potential false-positive findings in the pediatric population, nuclear medicine physicians and radiologists should exercise
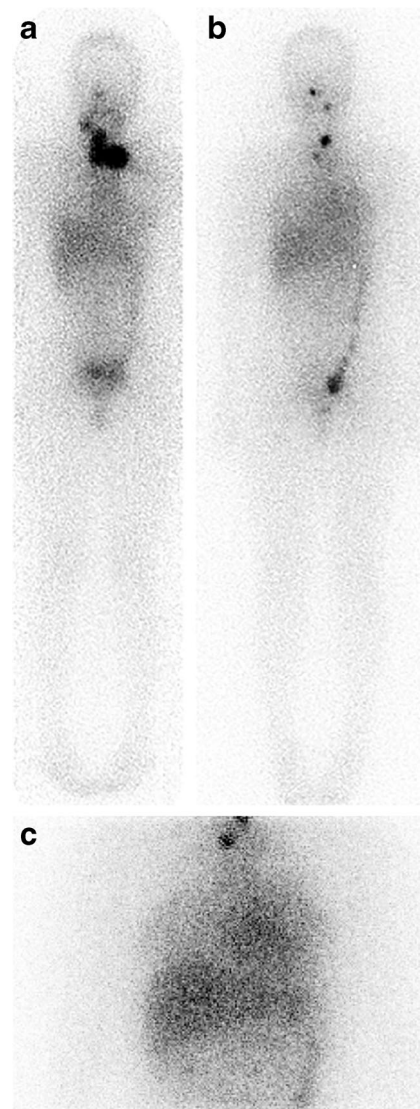
diligence when reviewing scans from this age group. This study is the first of its kind, to our knowledge, regarding the prevalence and detection of potential false-positive findings on radioiodine scans in children with differentiated thyroid carcinoma. Some studies and case reports have included a few children as part of their study cohort [3, 13]. Those reported findings can be extrapolated for comparison, based on the physiological, pathological or technical characteristics.

Ingested iodine is easily absorbed into the bloodstream and trapped by the thyroid follicular cells by the sodium-iodide symporter mechanism [14]. The iodine is then oxidized, organified and incorporated into the thyroglobulin molecule
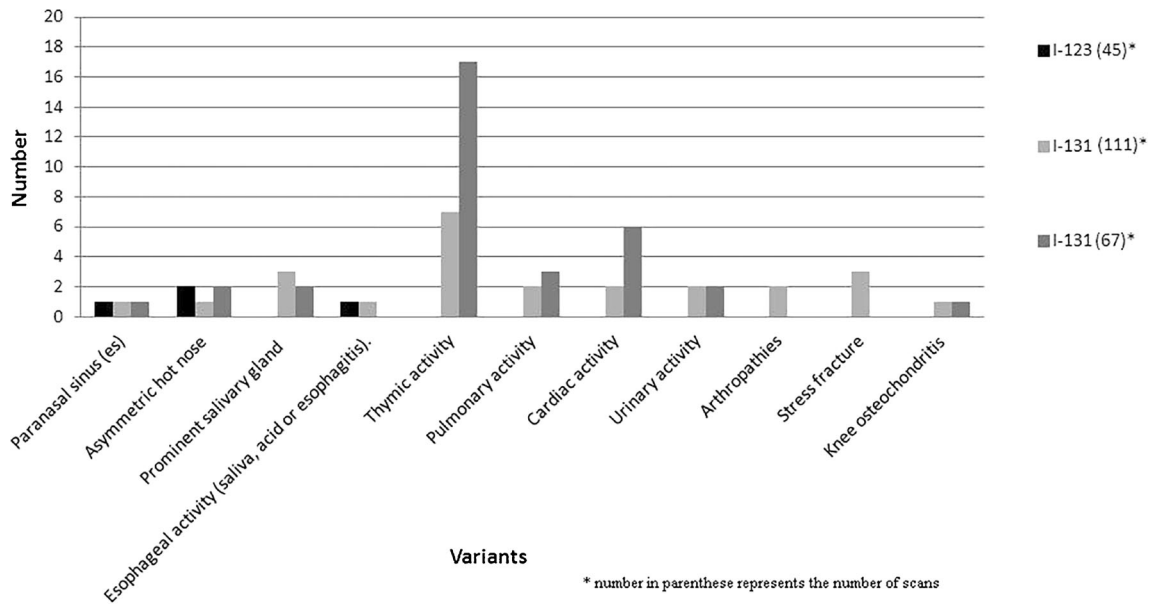
Fig. 4 Graph shows frequency of variants on 223 radioiodine scans of 53 children with differentiated thyroid cancer
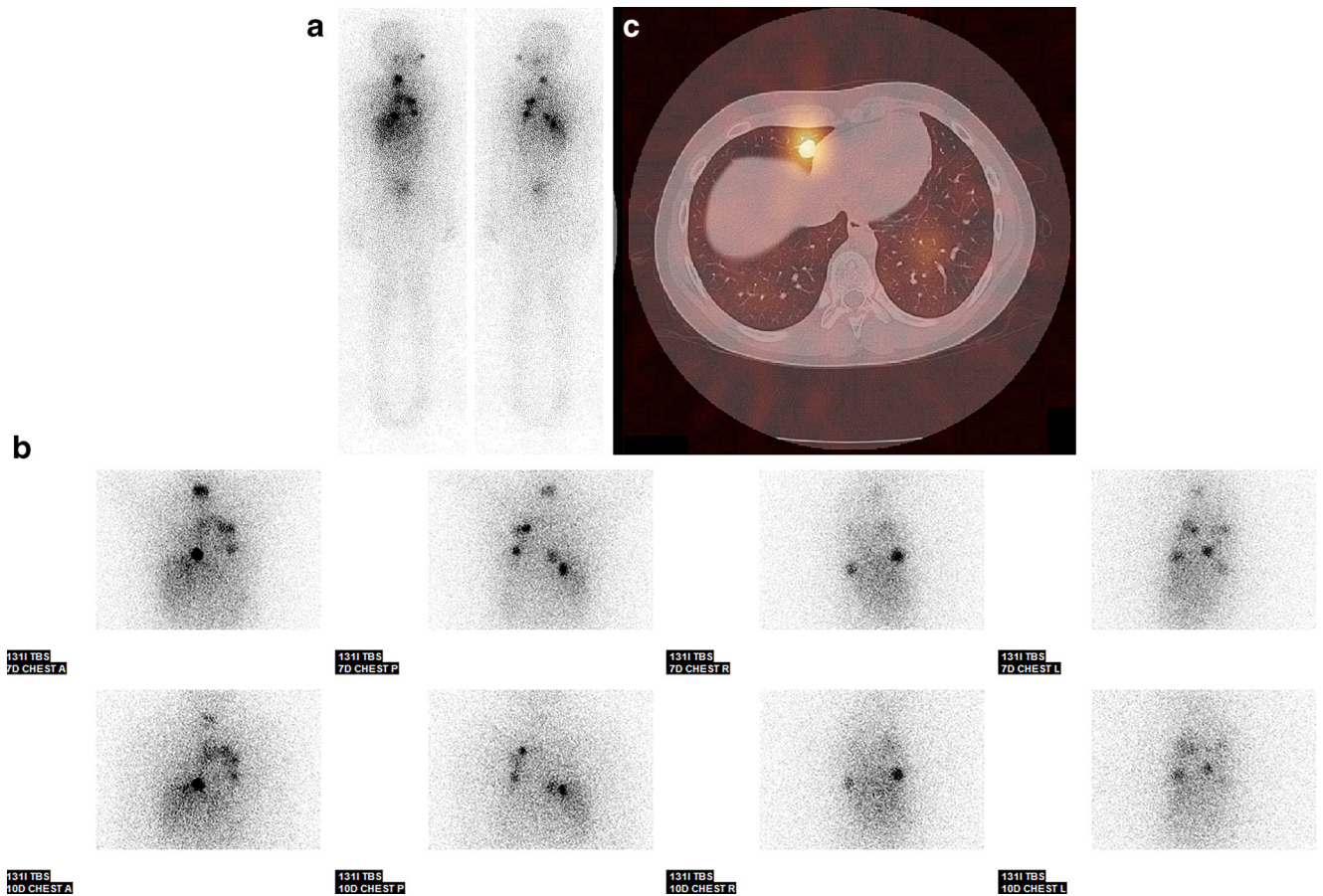

Fig. 5 Pulmonary activity. **a** Anterior and posterior whole-body scan 7 days after radioiodine therapy. **b** Spot views 7 and 10 days after radioiodine therapy (in anterior, posterior, right lateral and left lateral views) in a 15-year-old boy with differentiated thyroid cancer show multiple foci of activity in the chest region in addition to the neck uptake. On lateral views the lesions seem to be in the lungs (**b**). Single-photon emission computed tomography (SPECT) study confirmed the diagnosis (not shown). **c** Axial SPECT/CT fusion image correctly delineates a pulmonary lesion

Fig. 6 Star artifact caused by intense activity in the neck 8 days after radioiodine ablation therapy in a 12-year-old boy

to produce thyroid hormones [14]. Sodium-iodide symporter is also the main mechanism of uptake in the functioning thyroid cancer tissues [14–16]. The iodine in the bloodstream is excreted via the kidneys to the ureters and bladder. A small amount of iodine is also excreted into the colon and in sweat [16]. In the majority of cases, the pattern of radioiodine distribution in the whole-body iodine scan depends on these two mechanisms. Sodium-iodide symporter is also expressed in stomach, salivary and lacrimal glands and thymus, and probably to a lesser extent in lung, heart, prostate, ovary and adrenal glands [14–16]. The metabolism of the thyroglobulin molecule (or thyroid hormones) containing radioiodine in the liver might be another mechanism for visualization of liver after radioiodine therapy [16].

Visualization of the thymus on whole-body radioiodine scans has been frequently reported [17–20]. In a review of 175 patients, thymic uptake was observed on 7 whole–body radioiodine scans of 6 patients, including 1.2% (4/325) of diagnostic whole-body scans and 1.5% (3/200) of post-therapy whole-body scans [18]. In our study the most common variant was thymic activity, which was detected more on post-therapy whole-body scans, probably a result of higher doses of radioiodine compared with doses in diagnostic scans. The increased frequency of thymic activity in our study cohort as compared with the work of Davidson and McDougall [21] might be a result of the pediatric age of our study participants. Davidson and McDougall [21] reported that the mean age of their patients was 39 years (range 6–86 years) [21]. In our series, the mean age ± SD was 13 ± 2.3 years (range 9–17 years) upon initial scans. Steinmann [22] found that the thymic lymphoid component increases in size from birth
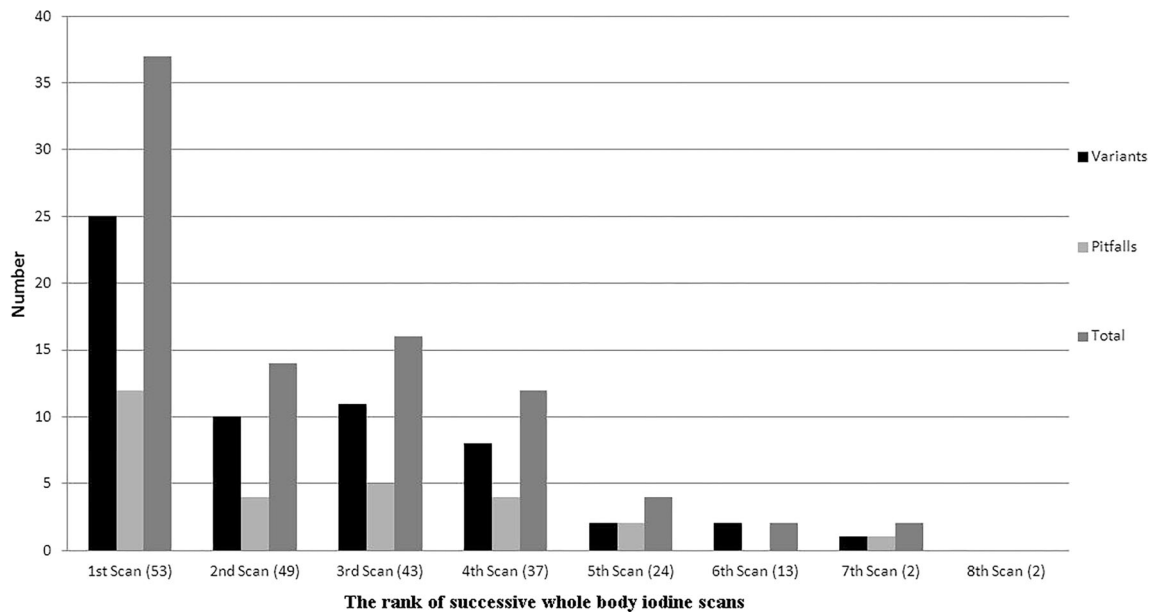

Fig. 7 Graph shows frequency of potential false-positive findings on successive whole-body radioiodine scans (total 178) in 53 children with differentiated thyroid cancer

to 20–25 years of age and then decreases progressively in size with further aging. The appearance of the thymus on whole-body radioiodine scans could be a result of the active thymic radioiodine uptake via sodium-iodide symporter [23–25].

Cardiac blood pool activity was noted on 6 of 67 (9%) post-therapy whole-body radioiodine scans in our study. Visualization of cardiac blood pool activity was seen in 33% (61/186) of post-ablation whole-body radioiodine scans reported by Aktas et al. [26]. They concluded that cardiac blood pool activity correlated with the intensity of residual thyroid uptake and had a significant association with increased thyroglobulin levels. The presence of a small quantity of sodium-iodide symporter in the heart might be another mechanism for

visualization of activity in the cardiac region [16]. In our study the two diagnostic whole-body scans showing cardiac blood pool activity were likely a result of slight cardiomegaly (Table 1). Lateral views (Fig. 8), delayed images and SPECT/CT (Fig. 5) might be helpful to differentiate cardiac blood pool activity caused by thymic uptake, physiological activity in breasts, or a functioning thyroid metastasis in the chest region.

Chest CT scan showed congruent basal bronchiectatic changes in three of the children in our study who had unexpected pulmonary activity on whole-body radioiodine scans. False-positive pulmonary radioiodine uptake caused by bronchiectasis has been reported [27, 28]. Recently Choi et al. [5]

Fig. 8 Whole-body iodine scan (anterior and posterior views) 7 days after radioiodine ablation therapy in a 16-year-old girl with differentiated thyroid cancer. **a** Scan in anterior projection shows considerable activity in the neck. There is also mild activity in the chest region and a focal radiotracer accumulation in the right upper quadrant. **b** Top row, on the lateral projection the activity in the chest seems to be related to physiological breast uptake (*arrow*). Spot views from abdomen in anterior and posterior projection (**b** middle row, *arrowhead*) confirm the presence of a focal uptake in the right upper quadrant. Delayed views in anterior and posterior projections (**b** bottom row) were obtained 3 days later (day 10 after therapy) to further investigate the possibility of radiotracer accumulation in the gastrointestinal tract in the right upper quadrant. The right upper quadrant activity was stable in the same location. Further investigation with US showed a cystic lesion in the right liver lobe (not shown). **c** The cystic lesion is stable on 1-year follow-up axial CT (as it was on US, not shown). **d** Follow-up whole-body iodine scan after 1 year shows no abnormal iodine-avid lesion. Thyroglobulin level was normal
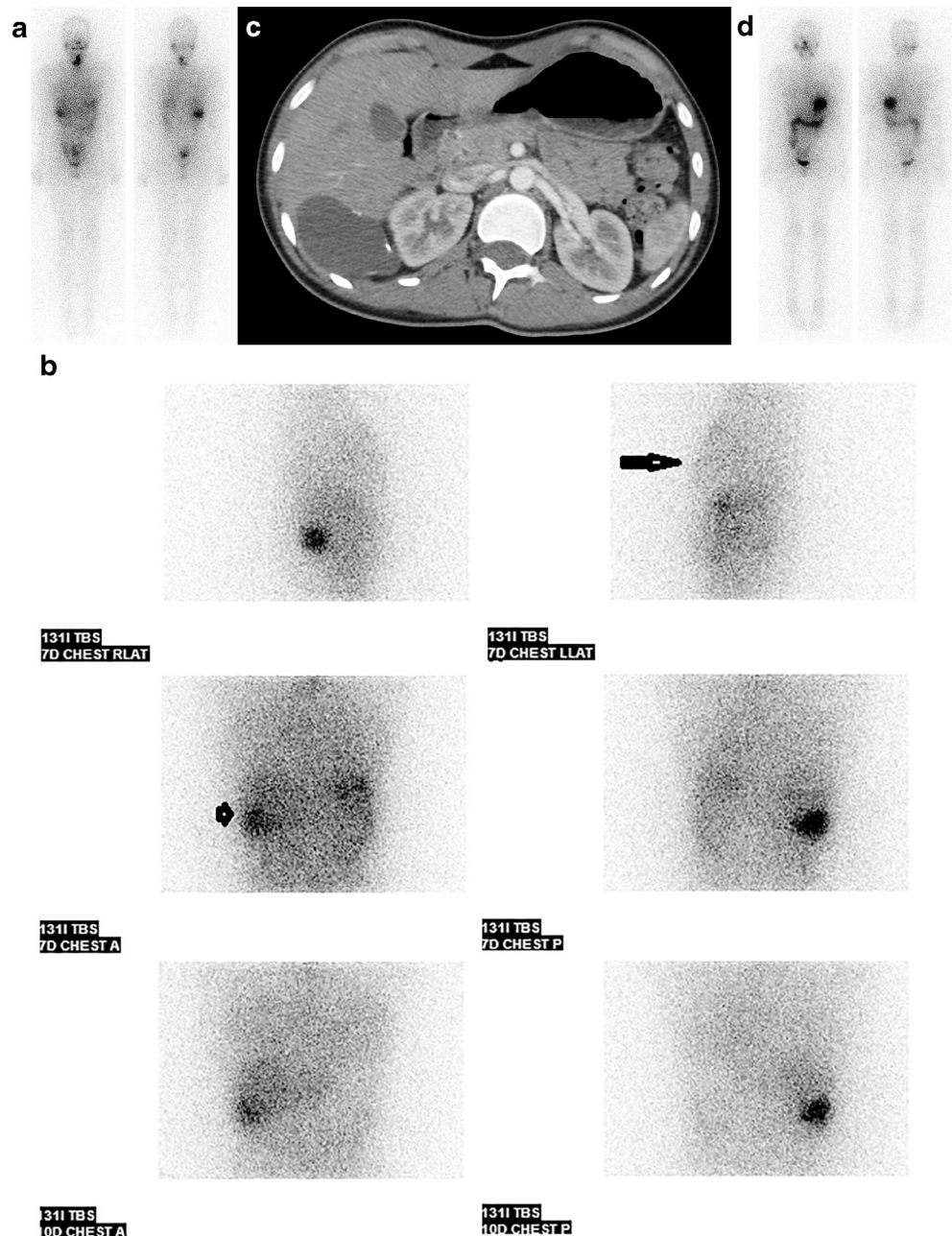
demonstrated that 22 of 755 (2.9%) post-therapy whole-body scans in patients with thyroid cancer (mean age 48.3 ± 9.2 years) revealed diffuse intrathoracic radioiodine uptake, without strict evidence of pulmonary metastases [5]. These authors verified the underlying pathologies by correlation with chest radiographs taken within 1 week or chest CT scans taken within 2 weeks. Pulmonary metastasis was confirmed on histology, by identification of nodules that enlarged during a minimum follow-up period of 6 months on chest radiographs or chest CT scans, or when findings of lung metastases were identified on radioactive iodine scans with elevated serum thyroglobulin levels (>2 ng/ml) on follow-up [5]. In their study, the age, gender and biochemical markers were matched among patients with positive indeterminate diffuse findings and those with negative intrathoracic uptake. Nevertheless such indeterminate pulmonary activity was more frequent in cases subjected to thyroid hormone withdrawal than recombinant TSH stimulation [5]. In our series, all children were subjected to thyroid hormone withdrawal. Diffuse indeterminate pulmonary activity — in absence of CT-revealed chest pathology — was demonstrated on 2 of 5 whole-body radioiodine scans with diffuse pulmonary activity (Table 1).

Accumulation of excreted radioiodine accounts for the focal activity at sites of nasal piercing, the esophagus and the extra-vesical urinary tract [1]. Transient or permanent narrowing or obstruction following radioiodine therapy can lead to asymmetrical salivary activity [3]. Increased capillary permeability has been suggested as the cause of increased focal radioiodine accumulation at inflamed sites [16]. Moreover, as part of their bactericidal effect, leukocytes are known to induce iodide organification by means of a myeloperoxidase [29]. Therefore retention of radioiodine in leukocytes of post-traumatic clots or tissues might also explain various reports of false-positive uptake at sites of inflammation [30, 31]. In agreement with such principles, this study showed focal increased radioiodine accumulation at inflamed paranasal sinuses, joints and stress fractures (Table 1).

Star artifact might be seen with higher doses of radioiodine because of septal penetration of the collimator holes. The number of points and the shape depends on the design of the collimator. Because of the hexagonal shape of most collimators, star artifact is typically seen as a six-point star in the region of high intense activity (Fig. 6). In our study star artifact was noted in 6 of 223 cases. Because of the intense focal uptake in the area of the star artifact, the pattern of activity cannot be demonstrated [32]. This artifact might limit evaluation of adjacent functioning thyroid metastasis (e.g., a small lymph node adjacent to the thyroid remnant tissue). Further imaging with a pinhole collimator resolves this artifact [32].

The frequency of thymic, cardiac and pulmonary activity was highest on post-therapy whole-body scans. This could be a result of different administered doses of radioiodine because most follow-up studies were obtained after the diagnostic dose of radioiodine. Furthermore, the star artifact from thyroid remnant is a common pitfall on post-therapy whole-body scans. In addition, finger contamination, probably from radioactive saliva, was more prevalent in early scans. The decrease in the frequency of contamination on the subsequent scans was likely a result of improved patient orientation prior to scanning. The decreased flow of saliva following radioiodine therapy might also be a contributing factor. Raza et al. [33] found that the maximum secretion and uptake ratio was decreased in 46% and 42% of patients, respectively, on sialoscintigraphy.

This study has several limitations because of its small sample size and retrospective nature. However, because thyroid cancer is a rare condition in children the sample size and the number of studies evaluated were acceptable to reach a conclusion. Multicenter studies are needed to address this issue. The protocols to acquire images might differ among pediatric centers. For example at some centers whole-body scan with I-123 is used for follow-up studies. In our protocol initial scans before therapy were done with I-123. The initial scans with I-123 in our protocol were obtained from the neck and upper chest area (not whole body) (Fig. 9). Therefore

Fig. 9 I-123 scan from neck and upper chest in a 16-year-old girl (a). An external source of activity (cobalt 67) was put behind the girl for better localization of the activity (b). The calculated neck uptake after 24 h showed a considerable remnant (20% neck uptake). The girl was operated again to minimize the neck uptake before radioiodine ablation therapy
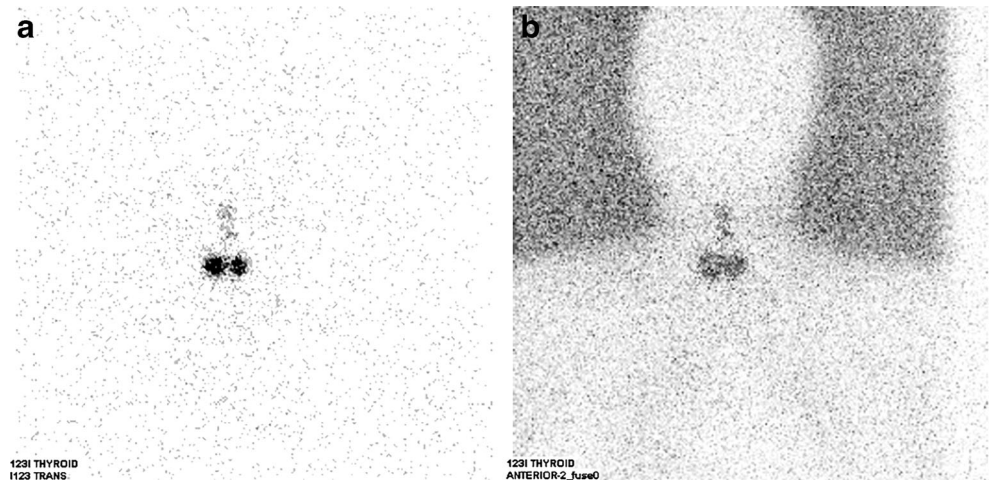
comparison of the pitfalls and variants between I-123 and I-131 were not possible in our study. As with any retrospective studies, management and imaging protocols might differ among patients; however at our hospital there is a well-established protocol for thyroid cancer management with regular follow-up diagnostic imaging scans, which minimizes this effect. Finally, it is worth mentioning that we used to acquire I-123 scans using a low-energy collimator; the quality of images would have been improved with a medium-energy collimator as opposed to a low-energy collimator because of less septal penetration of γ-rays.

Conclusion

Variants and pitfalls that mimic functioning thyroid tissue or functioning thyroid carcinomatous tissue on whole-body radioiodine scan in children with differentiated thyroid carcinoma are not infrequent; these do, however, decrease in frequency on successive whole-body radioiodine scans. Potential false-positive findings can be minimized with proper knowledge of the common variants and pitfalls in children and correlation with clinical, laboratory and imaging data.

Compliance with ethical standards

Conflicts of interest None

References

1. Shapiro B, Rufini V, Jarwan A et al (2000) Artifacts, anatomical, and physiological variants, and unrelated diseases that might cause false-positive whole-body 131-I scans in patients with thyroid cancer. Semin Nucl Med 30:115–132
2. Intenzo CM, Jabbour S, Dam HQ et al (2005) Changing concepts in the management of differentiated thyroid cancer. Semin Nucl Med 35:257–265
3. Glazer DI, Brown RKJ, Wong KK et al (2013) SPECT/CT evaluation of unusual physiologic radioiodine biodistributions: pearls and pitfalls in image interpretations. Radiographics 33: 397–418
4. Buton L, Morel O, Gault P et al (2013) False-positive iodine-131 whole-body scan findings in patients with differentiated thyroid carcinoma: report of 11 cases and review of literature. Ann Endocrinol 74:221–230
5. Choi HS, Kim SH, Park SY et al (2014) Clinical significance of diffuse intrathoracic uptake on post-therapy I-131 scans in thyroid cancer patients. Nucl Med Mol Imaging 48:63–71
6. Ozguven M, Ilgan S, Arslan N et al (2004) Unusual patterns of I-131 contamination. Ann Nucl Med 18:271–274
7. Omur O, Akgun A, Ozcan Z et al (2009) Clinical implications of diffuse hepatic uptake observed in postablative and post therapeutic I-131 scans. Clin Nucl Med 34:11–14
8. Biyi A, Oufroukhi Y, Doudouh A (2008) False-positive whole-body I-131 scan in thyroid carcinoma caused by gastrooesophageal

reflux disease. Internet J Nucl Med. https://nucleus.iaea.org/HHW/NuclearMedicine/Radioguided_Surgery_and_Radionuclide_Therapy/RadionuclideTherapy/Thyroidmalignant/TeachingCases/ThyroidTeacCases/For_Thyroid_Malig-_ATLAS_I131_False_Positives_.pdf. Accessed 10 May 2016
9. Blum M, Tiu S, Chu M et al (2011) I-131 SPECT/CT elucidates cryptic findings on planar whole-body scans and can reduce needless therapy with I-131 in post-thyroidectomy thyroid cancer patients. Thyroid 21:1035–1048
10. Francis GL, Waguespack SG, Bauer AJ et al (2015) Management guidelines for children with thyroid nodules and differentiated thyroid cancer. The American Thyroid Association Guidelines Task Force on Pediatric Thyroid Cancer. Thyroid 25:716–759
11. Shea KM (2009) Children and radiation. Children's health and the environment: WHO training package for the health sector. World Health Organization. http://www.who.int/ceh/capacity/radiation.pdf. Accessed 10 May 2016
12. Brenner DJ, Elliston CD, Hall EJ et al (2001) Estimated risk of radiation-induced fatal cancer from pediatric CT. AJR Am J Roentgenol 176:289–296
13. Van Nostrand D, Aiken M, Atkins F et al (2009) The utility of radioiodine scans prior to iodine 131 ablation in patients with well-differentiated thyroid cancer. Thyroid 19:849–855
14. Byeong-Cheol A (2011) Physiologic and false positive pathologic uptakes on radioiodine whole body scan. In: Gholamrezanezhad A (ed) 12 chapters on nuclear medicine. In Tech, Rijeka, pp 1–25
15. Chung JK (2002) Sodium iodide symporter: its role in nuclear medicine. J Nucl Med 43:1188–1200
16. Oh J-R, Ahn B-C (2012) False-positive uptake on radioiodine whole-body scintigraphy: physiologic and pathologic variants unrelated to thyroid cancer. Am J Nucl Med Mol Imaging 2: 362–385
17. Michigishi T, Mizukami Y, Shuke NK et al (1993) Visualization of the thymus with therapeutic doses of radioiodine in patients with thyroid cancer. Eur J Nucl Med 20:75–79
18. Vermiglio F, Baudin E, Travagli JP et al (1996) Iodine concentration by the thymus in thyroid carcinoma. J Nucl Med 37: 1830–1831
19. Wilson LM, Barrington SF, Morrison ID et al (1998) Therapeutic implications of thymic uptake of radioiodine in thyroid carcinoma. Eur J Nucl Med 25:622–628
20. Mello ME, Flamini RC, Corbo R et al (2009) Radioiodine concentration by the thymus in differentiated thyroid carcinoma: report of five cases. Arq Bras Endocrinol Metabol 53:874–879
21. Davidson J, McDougall IR (2000) How frequently is the thymus seen on whole-body iodine-131 diagnostic and post-treatment scans? Eur J Nucl Med 27:425–430
22. Steinmann GG (1986) Changes in the human thymus during aging. Curr Top Pathol 75:43–88
23. Meller J, Becker W (2000) The human sodium iodine symporter (NIS) as a key for specific thymic iodine-131 uptake. Eur J Nucl Med 27:473–474
24. Connolly LP, Connolly SA (2003) Thymic uptake of radiopharmaceuticals. Clin Nucl Med 28:648–651
25. Riesco-Eizaguirre G, Santisteban P (2006) A perspective view of sodium iodide symporter research and its clinical implications. Eur J Endocrinol 155:495–512
26. Aktas A, Kocabas B, Erhamamcı S et al (2015) Cardiac blood pool activity on postablation radioiodine imaging. Ann Nucl Med 29:170–176
27. Jong I, Taubman K, Schlicht S (2005) Bronchiectasis simulating pulmonary metastases on iodine-131 scintigraphy in well-differentiated thyroid carcinoma. Clin Nucl Med 30:688–689
28. Tsai D-H, Hsiao H-C, Tu S-T et al (2007) Concomitant false-positive and false-negative iodine-131 scintigraphy secondary to

bronchiectasis and cervical lymph node metastasis in a patient with thyroid cancer: the usefulness of FDG-PET/CT. Ann Nucl Med Sci 20:217–221

29. Klebanoff SJ, Hamon CB (1972) Role of myeloperoxidase-mediated antimicrobial systems in intact leukocytes. J Reticuloendothel Soc 12:170–196

30. Regalbuto C, Buscema M, Arena S et al (2002) False-positive findings on (131)I whole-body scans because of posttraumatic superficial scabs. J Nucl Med 43:207–209

31. Brucker-Davis F, Reynolds JC, Skarulis MC et al (1996) False-positive iodine-131 whole-body scans due to cholecystitis and sebaceous cyst. J Nucl Med 37:1690–1693

32. Wartofsky L, Van Nostrand D (2006) Thyroid cancer: a comprehensive guide to clinical management, 2nd edn. Humana Press, Totowa

33. Raza H, Khan AU, Hameed A et al (2006) Quantitative evaluation of salivary gland dysfunction after radioiodine therapy using salivary gland scintigraphy. Nucl Med Commun 27:495–499